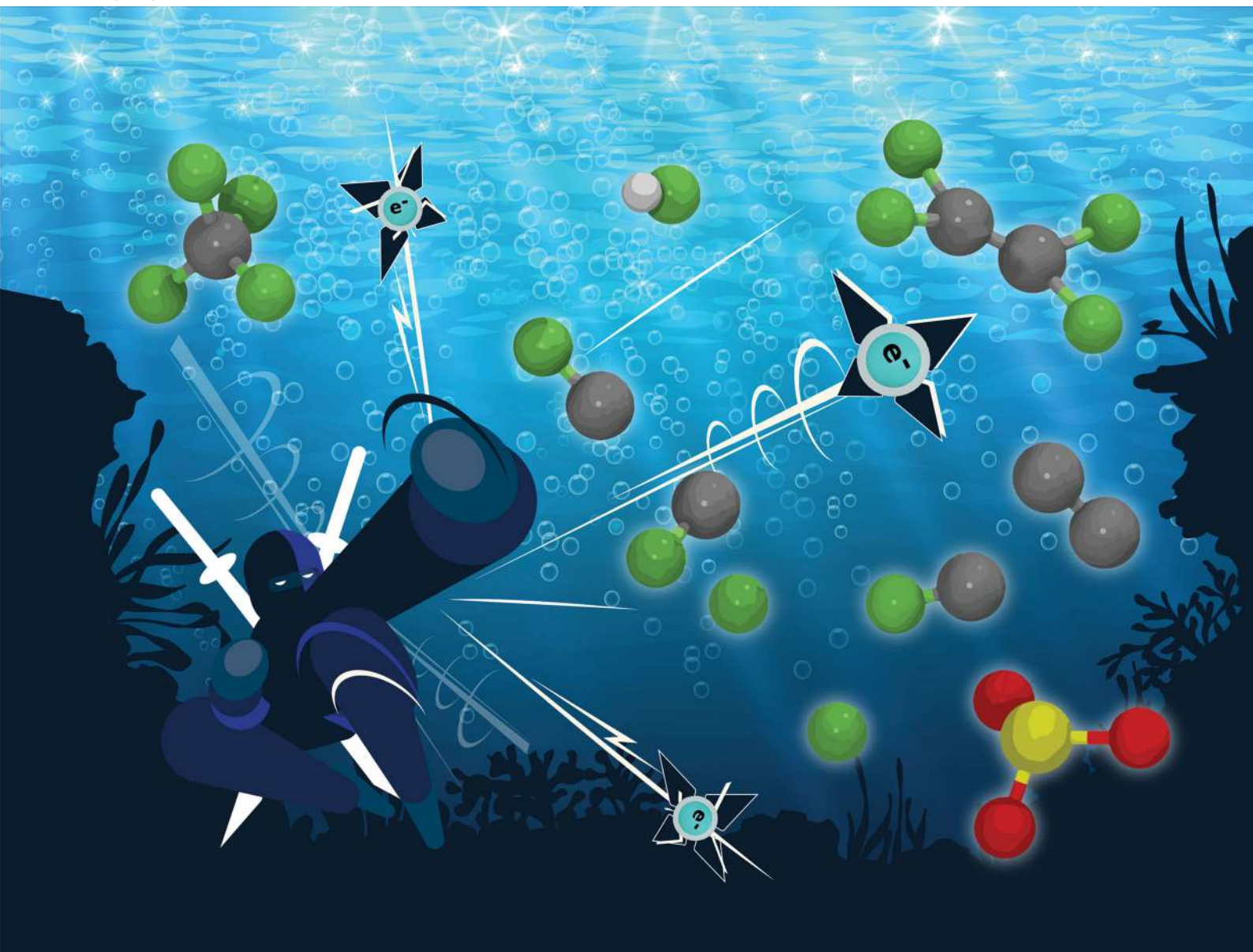


PCCP

Physical Chemistry Chemical Physics

rsc.li/pccp



ISSN 1463-9076

COMMUNICATION

Bryan M. Wong *et al.*
Real-time degradation dynamics of hydrated per- and
polyfluoroalkyl substances (PFASs) in the presence of
excess electrons


 Cite this: *Phys. Chem. Chem. Phys.*, 2020, 22, 6804

 Received 17th December 2019,
Accepted 21st January 2020

DOI: 10.1039/c9cp06797c

rsc.li/pccp

Real-time degradation dynamics of hydrated per- and polyfluoroalkyl substances (PFASs) in the presence of excess electrons†

 Sharma S. R. K. C. Yamijala,  Ravindra Shinde  and Bryan M. Wong *

Per- and polyfluoroalkyl substances (PFASs) are synthetic chemicals that are harmful to both the environment and human health. Using self-interaction-corrected Born–Oppenheimer molecular dynamics simulations, we provide the first real-time assessment of PFAS degradation in the presence of excess electrons. In particular, we show that the initial phase of the degradation involves the transformation of an alkane-type C–C bond into an alkene-type C=C bond in the PFAS molecule, which is initiated by the *trans* elimination of fluorine atoms bonded to these adjacent carbon atoms.

The strongest and most stable bond in organic chemistry is the carbon–fluorine (C–F) bond.¹ The high stability of this bond, which has enabled several technological advancements in the past century, now poses a serious health hazard.^{2–5} In the last century, the industrial sector has harnessed the intrinsic strength of the C–F bond to incorporate per- and polyfluoroalkyl substances (PFASs) in a wide variety of consumer and industrial goods.^{6–8} Specifically, PFASs are regularly used in the electronics, automotive, and aviation industries;^{6,7} several consumer goods, including non-stick cookware, clothing, carpets, shampoos, cleaning agents, and adhesives contain these persistent pollutants.⁸ As such, the wide-spread usage of these anthropogenic compounds has contaminated water resources in the US and many other countries.^{9–11} Most importantly, the subsequent consumption of this contaminated water leads to the bio-accumulation of these compounds in various organisms, including humans.^{9,10,12–14} In all of these examples, the intrinsic strength of the C–F bond in PFASs prevents most organisms from dissociating these compounds through natural means,¹⁵ which facilitates their bio-accumulation and toxicity. Thus, the intrinsic strength of the C–F bond poses a severe threat to many forms of life, making the treatment of these contaminated water sources essential.

An efficient treatment often includes either direct *in situ* destruction or removal of PFASs from contaminated water (for example, using sorption or nanofiltration) and their subsequent destruction in the wastewater concentrate.^{16,17} Since per- and polyfluoroalkyl compounds primarily contain C–C and C–F bonds, the degradation of PFASs requires the dissociation of both of these bonds. However, breaking a C–C bond is less effective than C–F bond cleavage,^{16,17} since the former generates short-chain PFASs that are still found to be toxic.^{18,19} Thus, the primary challenge in the complete treatment of PFAS-contaminated water is the efficient dissociation of the strong C–F bonds in these pollutants.

In the scientific literature, a few studies have suggested possible avenues for C–F bond dissociation in the presence of additional electrons.^{20–22} However, the majority of these studies carried out their analysis after the degradation has occurred, and specific mechanistic details of PFAS degradation are less understood. Although a few computational studies have addressed possible degradation of PFASs with excess electrons,²⁰ these studies were limited to static (*i.e.*, non-dynamic or stationary) electronic structure methods. As such, these prior approaches restrict our understanding of PFAS degradation dynamics. Also, to the best of our knowledge, there is little or no information on defluorination timescales in PFASs. To bridge this significant knowledge gap, we carried out extensive first-principles Born–Oppenheimer Molecular Dynamics (BOMD) simulations on both perfluorooctanoic acid (PFOA) and perfluorooctanesulfonic acid (PFOS) molecules (the most common PFAS contaminants in the environment) in the presence of explicit water molecules. While we find these pollutants to be stable in neutral aqueous environments, our results indicate that both of these molecules readily defluorinate at ultrafast timescales (<100 fs) in the presence of excess electrons. By considering a variety of different initial conditions, we unambiguously show that defluorination in PFASs often leads to the formation of an intermediate with an alkene type C=C bond, which is crucial in the degradation of PFASs. In addition, we also show that the formation of an HF molecule is a possible outcome of the BOMD simulations. As such, this work

Department of Chemical & Environmental Engineering, Materials Science & Engineering Program, and Department of Physics & Astronomy, University of California, Riverside, CA 92521, USA. E-mail: bryan.wong@ucr.edu;
Web: <http://www.bmwong-group.com>

† Electronic supplementary information (ESI) available: Computational details and supporting data. See DOI: 10.1039/c9cp06797c

provides detailed mechanistic insight and presents the first real-time picture of degradation dynamics of PFASs in the presence of excess electrons.

Inspired by recent works demonstrating that reduction processes (*i.e.*, the addition of electrons) can degrade PFASs,^{20–22} we studied the degradation dynamics of both PFOA and PFOS in the presence of excess electrons. To avoid any spurious self-interaction effects, which are usually observed with semi-local functionals such as PBE, we have included self-interaction corrections in all our MD simulations (further details are given in the ESI†). To mimic the water environment, we solvated each of these PFASs with 43 explicit water molecules. Due to this explicit solvent environment, both PFOA and PFOS lose their acidic proton to water molecules (as they should) during the *NVT* equilibration. In Fig. 1, we present the geometries of PFOA and PFOS molecules (top and bottom panels, respectively) after a 1 ps-long *NVE* simulation carried out with a different number of excess electrons. In the left panel, we show our results with no additional charge. As expected, both PFOA and PFOS were stable (*i.e.*, no bond dissociation) during the entire simulation time. In contrast, for simulations containing excess electrons, we observed an apparent degradation of these molecules. In the middle and right panels of Fig. 1, we show our results with -1 and -2 electronic charges, respectively. Both PFOA and PFOS were defluorinated in the presence of excess electrons, and we find that the number of dissociated C–F bonds is proportional to the number of additional electrons in the simulation box. We verified the robustness of these results by simulating six different initial conditions (*i.e.*, positions and velocities) for both PFOA and PFOS (*i.e.*, an additional 12 *NVE* simulations), and these results are shown in Fig. S1 and S2 in the ESI.† The initial conditions for all these additional runs were obtained from a 10 ps-long *NVT* equilibration run, and a C–F bond dissociation was observed in all these simulations. Collectively, these results

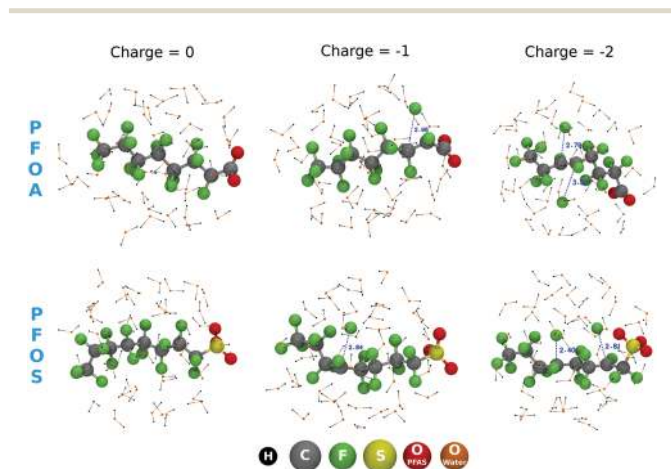


Fig. 1 Geometries of hydrated PFOA (top panel) and PFOS (bottom panel) molecules after a 1 ps long *NVE* run with 0 (left), 1 (middle), and 2 (right) excess electrons. For both molecules, we observe defluorination in the presence of excess electrons. We verified the robustness of these results by simulating six different initial conditions for both PFOA and PFOS (*i.e.*, an additional 12 *NVE* simulations), which are shown in Fig. S1 and S2 in the ESI.†

demonstrate that “excess electrons” can dissociate the crucial C–F bonds in per- and polyfluoroalkyl substances to facilitate their degradation.

Next, we examined the defluorination timescales in both PFOA and PFOS molecules with excess electrons. The initial conditions for all our *NVE* runs were taken from *NVT* calculations of neutral systems, with excess electrons subsequently added to simulate the dynamics of electrostatically charged environments. That is, the first frame of all the *NVE* runs correspond to the neutral (*i.e.*, uncharged) geometries. For each of the dissociated C–F bonds shown in Fig. 1, we studied the dissociation dynamics as a function of time, which are presented in Fig. 2. Clearly, at the beginning of all these simulations, the C–F bond distance is slightly larger than 1.3 Å, which is approximately the equilibrium C–F bond distance in neutral PFASs. At the end of these simulations, the bond distance increased to 3 Å, suggesting a complete dissociation of these C–F bonds in the presence of excess electrons. However, interestingly, in all these simulations, the C–F bond dissociation occurred within the first 100 fs (see the insets of different panels in Fig. 2). Here, it is essential to note that

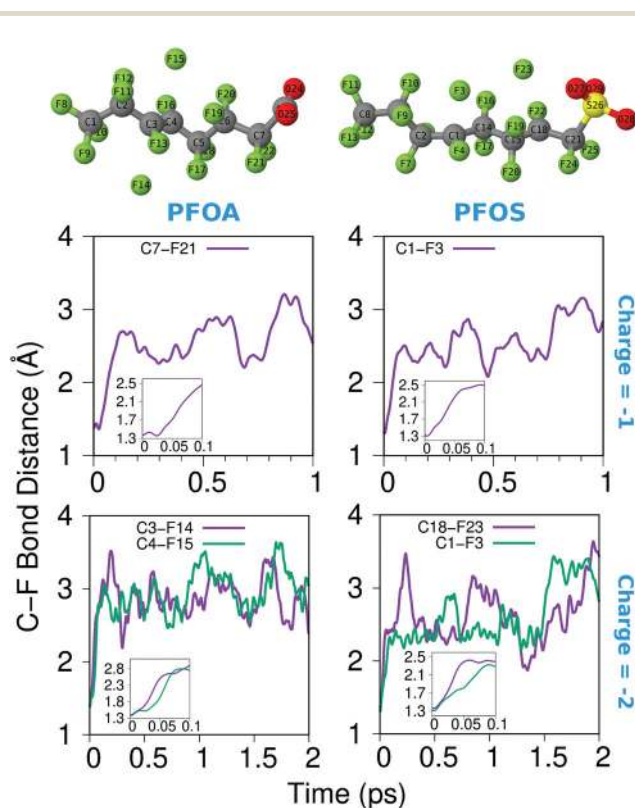


Fig. 2 Bond distance profiles of the dissociated C–F bonds for the structures shown in Fig. 1. Results with -1 (middle panel) and -2 (bottom panel) electronic charges are presented for both PFOA (top left) and PFOS (top right) molecules. The insets in each panel show the variation in the C–F bond distances during the first 100 fs ($= 0.1$ ps) of the simulations. In all our simulations, we observed the dissociation of C–F bonds in less than 100 fs (*i.e.*, an ultrafast dissociation). The legends in the figure designate the dissociated C–F bonds, and the corresponding atom numbering scheme is shown in the top panel. The structures in this panel were obtained after a 1 ps *NVE* simulation containing a -2 electronic charge (water molecules were omitted for clarity).

the dissociated C–F bonds in the PFOA and PFOS molecules are different, and even the dissociated C–F bonds in PFOA for the -1 and -2 electronic charges also differ (note the legends and top panel of Fig. 2 for the various dissociated C–F bonds). Despite these variations, we consistently observed an ultrafast degradation (*i.e.*, <100 fs) of PFASs in all these simulations. Furthermore, we verified this ultrafast dissociation of C–F bonds in all the other 12 *NVE* simulations (see the ESI[†]). Thus, we note that excess electrons not only facilitate C–F bond dissociation in PFASs, but also initiate this process on an ultrafast timescale.

In Fig. 3, we show the evolution of the spin-density as a function of time for both PFOA and PFOS with -1 and -2 electronic charges. We note that the LUMO of neutral hydrated PFOA and PFOS is localized entirely on the PFAS molecule (*i.e.*, not on water); as such, the addition of an electron to this composite system is expected to fill this unoccupied orbital on PFAS. Indeed, as shown in the top panel of Fig. 3, the additional charge (more precisely, spin) initially delocalizes on the entire PFOA molecule; however, as the simulation proceeds, the spin slowly accumulates at the site of dissociation. We also obtained similar results with the PFOS molecule (see Fig. S3, ESI[†]) as well as in four additional *NVE* calculations performed with a -1 electronic charge (not shown). These four calculations are different from the 12 *NVE* calculations presented in the ESI[†].

In a previous study on excess electrons,²⁰ Su and co-workers were unable to assign the initial site of the degradation process through their electronic structure calculations. In all our simulations, we also find that the site of dissociation is arbitrary. However, our spin-density results provide additional reasoning for Su and co-workers' observation. First, since the excess electron initially delocalizes over the entire PFAS molecule, all the C–F bonds are weakened and have an almost equal probability for dissociation. The specific C–F bond that dissociates during the simulation is thus arbitrary and is most possibly triggered by interactions between the contaminant and the solvent (here, PFAS and water).

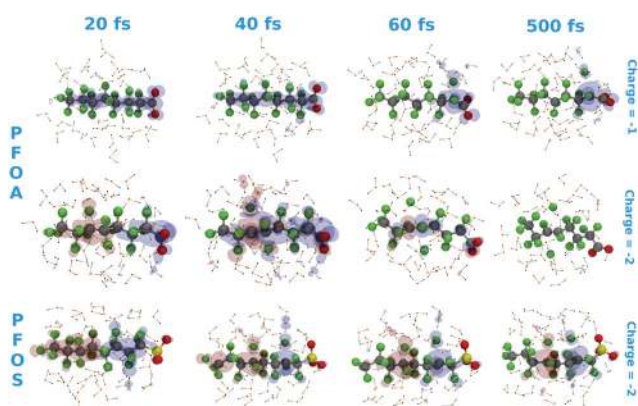


Fig. 3 Evolution of spin-density as a function of time for both the PFOA and PFOS molecules with excess electrons. PFOA with a -1 (-2) electronic charge is shown in the top (middle) panel, and PFOS with a -2 charge is shown in the bottom panel. The spin density of PFOS with a -1 electronic charge (not shown for brevity) is similar to the top PFOA panel (see Fig. S3, ESI[†]). An iso-value of 0.001, 0.00001, and 0.001 $e \text{ \AA}^{-3}$ was used for the top, middle, and bottom panels, respectively.

Next, although we mentioned that the site of dissociation is random, we never observed the dissociation of fluorine atoms attached to the terminal (primary) carbon atoms in any of our sixteen *NVE* simulations. This facile dissociation of secondary C–F bonds is due to their lower bond dissociation energy compared to the primary C–F bonds, as noted in a few earlier studies.^{23,24}

Contrary to the addition of a single electron, we find that the spin-density can evolve in two different ways with the addition of multiple electrons, as shown in the middle and bottom panels of Fig. 3. We refer to these different regimes as a *trans*-type (middle panel) or *cis*-type elimination (bottom panel) based on how the fluorine atoms have dissociated from the PFAS backbone structure. In both cases, initially, the spin-density of each additional electron is localized at different parts of the PFAS (*i.e.*, either towards the head or tail group), introducing a net spin-polarization in these compounds. However, as the simulation proceeds, this spin-polarization is either retained (*cis*-type) or completely suppressed (*trans*-type) depending on whether the dissociated fluorine atoms were bonded to adjacent carbon atoms or otherwise. As further demonstrated below, the spin-polarization quickly (<100 fs) decays when fluorine atoms dissociate from adjacent carbon atoms, due to the formation of a double bond between these carbon atoms (in other cases, the spin polarization is retained).

In Fig. 4, we present dynamical plots of atoms exhibiting maximum changes in the Mulliken charge and spin during the initial stages of the simulations (*i.e.*, during the C–F bond dissociation). Primarily, the charge profiles of both PFOA and PFOS with 2 excess electrons (Fig. 4A and C) show that the fluorine atoms captured these excess charges during the simulation. As such, there are no significant differences in the charge profiles for both *cis* and *trans*-type eliminations. Even in the simulations with a -1 electronic charge, we find that the excess charge is primarily localized on the fluorine atoms, and the carbon atoms retain the electronic spin (see Fig. S4, ESI[†]). In contrast to the charge profiles, the difference between the *cis* and *trans*-type eliminations manifests strongly in the spin profiles. In the *cis*-type elimination (Fig. 4D), opposite spins were localized on different carbon atoms (C1 and C18); in contrast, for the *trans*-type elimination, no atom is spin-polarized at the end of the simulation, which leads to the formation of a C=C bond along the PFAS backbone. Although the total residual spin is zero in both *cis* and *trans*-type eliminations, the *cis*-type elimination produces an antiferromagnetic intermediate, and a *trans*-type elimination results in a non-magnetic intermediate. This behaviour was confirmed in all the 16 *NVE* simulations performed with 2 excess electrons.

Since we observed a *trans*-type elimination in most of our simulations (12 out of 16), we suggest that this intermediate could be central to the degradation of per- and polyfluoroalkyl substances. A few recent experiments further support this finding. For example, Liu *et al.* have shown that fluorine atoms attached to a C=C bond (*i.e.*, sp^2 carbon atoms) dissociate more readily compared to fluorine atoms attached to a C–C bond (sp^3 carbon atoms).²³ Since most of our simulations with excess electrons resulted in a *trans*-type elimination with the formation of a C=C bond (which is known to be more susceptible

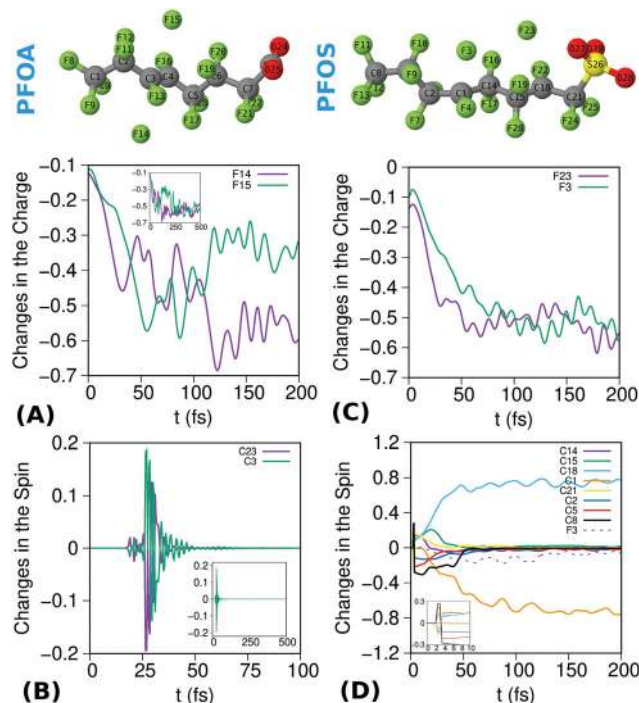


Fig. 4 Atoms exhibiting the largest changes in Mulliken charges (A and C) and spin (B and D) during the initial stages of the simulation (*i.e.*, during C–F bond dissociation). The left (right) panel depicts results for a PFOA (PFOS) molecule with two excess electrons. In both cases, after the C–F bond dissociation, negative charges were localized on the fluorine atoms. For only the *cis*-type elimination (see text for details), spins were localized on the carbon atoms (panel D). In the inset of panel A (B), the charge (spin) on the dissociated fluorine atoms are shown until 500 fs. In the inset of panel D, changes in the spin during the first 10 fs of the simulation are depicted. The atom numbering scheme is presented in the top panel.

to defluorination), we infer that this *trans*-type intermediate plays a crucial role in PFAS defluorination, which could explain the PFAS degradation (with excess electrons) observed by Su *et al.*²⁰ Apart from the *trans*-type intermediate, we also found that an HF molecule was formed during our simulations (see Fig. S5 and the ESI† for further details).

In conclusion, we have presented the first real-time, dynamical study of PFAS degradation with excess electrons to elucidate defluorination timescales and mechanisms. Using several large-scale *ab initio* trajectory calculations (16 different *NVE* simulations), we show that excess electrons enable the dissociation of the strongest C–F bonds in these contaminants, which occurs on an ultrafast timescale (<100 fs). Moreover, these large-scale simulations provide new mechanistic insight into PFAS degradation processes that manifest themselves strongly as spin and charge fluctuations as a function of time. In particular, we have shown that a *trans*-type C–F elimination (which leads to the formation of a C=C bond along the PFAS backbone) is more probable compared to a *cis*-type elimination. Since fluorine atoms attached to a C=C bond are more readily dissociated, this *trans*-type intermediate could play a central role in accelerating further PFAS defluorination processes. In addition, our dynamics simulations also show the spontaneous formation of

an HF molecule, which could be another significant intermediate/product of the PFAS degradation process. Taken together, these first-principles-based molecular dynamics show that (1) the use of excess electrons can be a viable approach for breaking the strongest C–F bonds in PFAS contaminants, and (2) the application of dynamical computational techniques can provide essential mechanistic insight (such as degradation timescales and short-lived intermediates) that cannot be readily gleaned from static electronic structure studies of PFAS or other aqueous contaminants.

Conflicts of interest

There are no conflicts to declare.

Acknowledgements

Self-interaction-corrected density functional theory calculations were supported by the U.S. Department of Energy, Office of Science, Early Career Research Program under Award No. DE-SC0016269. Born–Oppenheimer Molecular Dynamics simulations of PFAS contaminants were supported by the National Science Foundation under Grant No. CHE-1808242.

Notes and references

- 1 D. O'Hagan, *Chem. Soc. Rev.*, 2008, **37**, 308–319.
- 2 E. M. Sunderland, X. C. Hu, C. Dassuncao, A. K. Tokranov, C. C. Wagner and J. G. Allen, *J. Expo. Sci. Environ. Epidemiol.*, 2019, **29**, 131–147.
- 3 G. Goldenman, M. Fernandes, M. Holland, T. Tugran, A. Nordin, C. Schoumacher and A. McNeill, The cost of inaction: A socioeconomic analysis of environmental and health impacts linked to exposure to PFAS, Nordic Council of Ministers, 2019.
- 4 <https://pfas-1.itcreweb.org>.
- 5 P. Grandjean and R. Clapp, *New Solut.*, 2015, **25**, 147–163.
- 6 E. Kissa, *Fluorinated Surfactants and Repellents*, 2nd edn, CRC Press, 2001.
- 7 B. Ameduri and H. Sawada, *Fluorinated Polymers: Volume 2: Applications*, Royal Society of Chemistry, 2016.
- 8 M. Kotthoff, J. Müller, H. Jüriling, M. Schlummer and D. Fiedler, *Environ. Sci. Pollut. Res. Int.*, 2015, **22**, 14546–14559.
- 9 R. Bossi, M. Dam and F. F. Rigét, *Chemosphere*, 2015, **129**, 164–169.
- 10 A. Cordner, V. Y. De La Rosa, L. A. Schaidler, R. A. Rudel, L. Richter and P. Brown, *J. Exposure Sci. Environ. Epidemiol.*, 2019, **29**, 157–171.
- 11 J. S. Boone, C. Vigo, T. Boone, C. Byrne, J. Ferrario, R. Benson, J. Donohue, J. E. Simmons, D. W. Kolpin, E. T. Furlong and S. T. Glassmeyer, *Sci. Total Environ.*, 2019, **653**, 359–369.
- 12 K. Kannan, *Environ. Chem.*, 2011, **8**, 333–338.
- 13 K. Kannan, S. Corsolini, J. Falandysz, G. Fillmann, K. S. Kumar, B. G. Loganathan, M. A. Mohd, J. Olivero, N. Van Wouwe, J. H. Yang and K. M. Aldoust, *Environ. Sci. Technol.*, 2004, **38**, 4489–4495.

- 14 L. W. Y. Yeung, M. K. So, G. Jiang, S. Taniyasu, N. Yamashita, M. Song, Y. Wu, J. Li, J. P. Giesy, K. S. Guruge and P. K. S. Lam, *Environ. Sci. Technol.*, 2006, **40**, 715–720.
- 15 J. S.-C. Liou, B. Szostek, C. M. DeRito and E. L. Madsen, *Chemosphere*, 2010, **80**, 176–183.
- 16 N. B. Saleh, A. Khalid, Y. Tian, C. Ayres, I. V. Sabaraya, J. Pietari, D. Hanigan, I. Chowdhury and O. G. Apul, *Environ. Sci.: Water Res. Technol.*, 2019, **5**, 198–208.
- 17 K. H. Kucharzyk, R. Darlington, M. Benotti, R. Deeb and E. Hawley, *J. Environ. Manage.*, 2017, **204**, 757–764.
- 18 National Toxicology Program, DOI: 10.22427/ntp-tox-97.
- 19 National Toxicology Program, DOI: 10.22427/ntp-tox-96.
- 20 Y. Su, U. Rao, C. M. Khor, M. G. Jensen, L. M. Teesch, B. M. Wong, D. M. Cwiertny and D. Jassby, *ACS Appl. Mater. Interfaces*, 2019, **11**, 33913–33922.
- 21 S. Huang and P. R. Jaffé, *Environ. Sci. Technol.*, 2019, **53**, 11410–11419.
- 22 R. K. Singh, S. Fernando, S. F. Baygi, N. Multari, S. M. Thagard and T. M. Holsen, *Environ. Sci. Technol.*, 2019, **53**, 2731–2738.
- 23 J. Liu, D. J. Van Hoomissen, T. Liu, A. Maizel, X. Huo, S. R. Fernández, C. Ren, X. Xiao, Y. Fang, C. E. Schaefer, C. P. Higgins, S. Vyas and T. J. Strathmann, *Environ. Sci. Technol. Lett.*, 2018, **5**, 289–294.
- 24 A. Raza, S. Bardhan, L. Xu, S. S. R. K. C. Yamijala, C. Lian, H. Kwon and B. M. Wong, *Environ. Sci. Technol. Lett.*, 2019, **6**, 624–629.